Supplemental Information

Long-term reprogramming of classical monocytes with altered ontogeny mediates enhanced lung injury in sepsis survivors

Scott J. Denstaedt, Breanna McBean, Alan P. Boyle, Brett C. Arenberg, Matthias Mack, Bethany B. Moore, Michael W. Newstead, Yamei Deng, Alexey I. Nesvizhskii, Benjamin H. Singer, Jennifer Cano, Hallie C. Prescott, Helen S. Goodridge, Rachel L. Zemans

Table of Contents

Supplemental Data		Page
Methods	Supplementary Methods	2
Figure S1	3-wk post-CLP baseline injury and inflammation	3
Figure S2	Exudate monocyte/macrophage flow cytometry panel	4
Figure S3	Exudate monocyte/macrophage depletion efficacy	5
Figure S4	BAL inflammation after monocyte depletion	6
Figure S5	Validation of monocyte adoptive transfer	7
Figure S6	BAL inflammation after monocyte adoptive transfer	8
Figure S7	Monocyte supernatant degranulation makers	9
Figure S8	3-mo post-CLP baseline injury and inflammation	10
Figure S9	Bone marrow monocyte and progenitor flow sorting panel	11
Figure S10	Control monocyte ATACseq – pathway enrichment	12
Figure S11	Post-CLP bone marrow monocyte characterization	13
Figure S12	Myeloid progenitor flow quantification	14
Figure S13	Consort diagram VA sepsis patient cohort	15
Figure S14	Conserved human-mouse monocyte subset signature	16
Figure S15	Monocyte purity after negative selection	17
Figure S16	Principle Component Analysis Ly6C^{hi} monocyte RNAseq	18
Table S1	Characteristics of Sepsis Cohort	19
Table S2	Sepsis hospitalization identification criteria	20
Table S3	Patient laboratory values after trimming non-physiologic data	21
Table S4	Patient laboratory values after trimming top and bottom 1%	21
References	References	22

Supplementary Methods

RNA-sequencing and analysis

RNA quality was assessed using a bioanalyzer (Agilent) and all RIN were greater than 7. Library preparation, sequencing, and identification of transcript frequency were performed by the University of Michigan Advanced Genomics Core. Library preparation was performed using the low input SMARTer smRNA-Seq kit (Takara). Samples were subjected to 151bp paired-end sequencing, with an average of 30-40 million reads per sample, according to the manufacturer's protocol (Illumina NovaSeq). BCL Convert Conversion Software (v3.9.3, Illumina) was used to generate de-multiplexed Fastq files. The reads were trimmed using *Cutadapt* (v2.3) (1). The reads were evaluated with *FastQC* (v0.11.8, Babraham Bioinformatics) to determine quality of the data. Reads were mapped to reference genome GRCm38 (ENSEMBL 102), using *STAR* (v2.7.8a) (2) or *HISAT2* (v 2.1.0) (3). Count estimates performed with *RSEM* (v1.3.3) (4) or *htseq-count* (version 0.13.5) (5). Alignment options followed ENCODE standards for RNA-seq. Differential gene expression analysis was conducted with *DESeq2* (version 1.38.3) (6), followed by pathway analysis using *pathfindR* (v1.6.4) (7). Differentially expressed genes (DEG) were identified at FDR p-value <0.05 and 1.25 fold-change. DEG and pathways available in the Genomic Data Supplement.

ATAC-sequencing and analysis

Cell suspensions were brought to the University of Michigan Advanced Genomics Core for library preparation using the Omni-ATAC-Seq protocol (8). Libraries were cleaned using MinElute (Qiagen) columns and AMPure XP beads (Beckman Coulter) before quantitation with the Qubit HS dsDNA kit (ThermoFisher), and quality assessment on a TapeStation HS D1000 kit (Agilent). The libraries were pooled and quantitated by qPCR using a Library Quantitation Kit – Illumina Platforms (KAPA) before sequencing on a NextSeq2000 P3 flow cell with an average of 100 million reads per sample. Sample quality was assessed by *FastQC* (v0.11.8, Babraham Bioinformatics). We aligned reads to mm10 with *HISAT2* (v2.1.0)(3). Filtering steps are performed with *samtools* (v1.2) (9).Unmapped reads and alignments below a MAPQ threshold were removed. Reads in blacklisted regions (ENCODE Blacklist Regions) were removed using *bedtools* (v2.28.0) (10). *F-Seq2* was used to call sample-wise peaks (v2.0.3) (11). Peaks over all samples are merged with *bedtools,* keeping peaks that occurred in at least 3 samples within a treatment group. Mitochondrial reads were filtered out. Differential peak analysis and pathway enrichment performed using the polyenrich function in *chipenrich* (v2.22.0) (12). Promoter- and enhancer-specific peaks were determined in R from polyenrich output, <|1000| dist_to_tss and >|1000| dist_to_tss, respectively. Motif enrichment analysis performed using Simple Enrichment Analysis package (*SEA*; v5.5.4) (13). Finding Individual Motif Occurrences (*FIMO*; v5.5.4) was used to assess AP-1 specific motif enrichment (14).

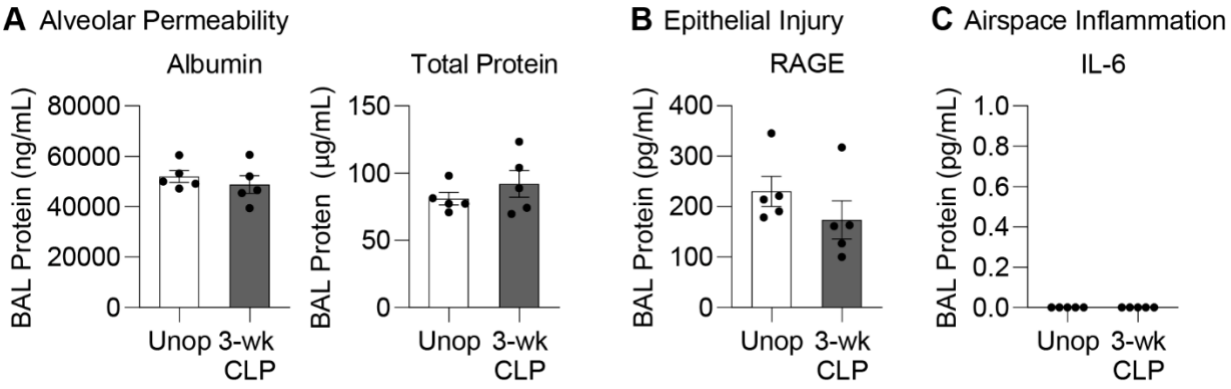


Figure S1. Baseline lung injury and inflammation 3 weeks post-CLP. BAL alveolar permeability (A), epithelial injury (B), and airspace inflammation (C).

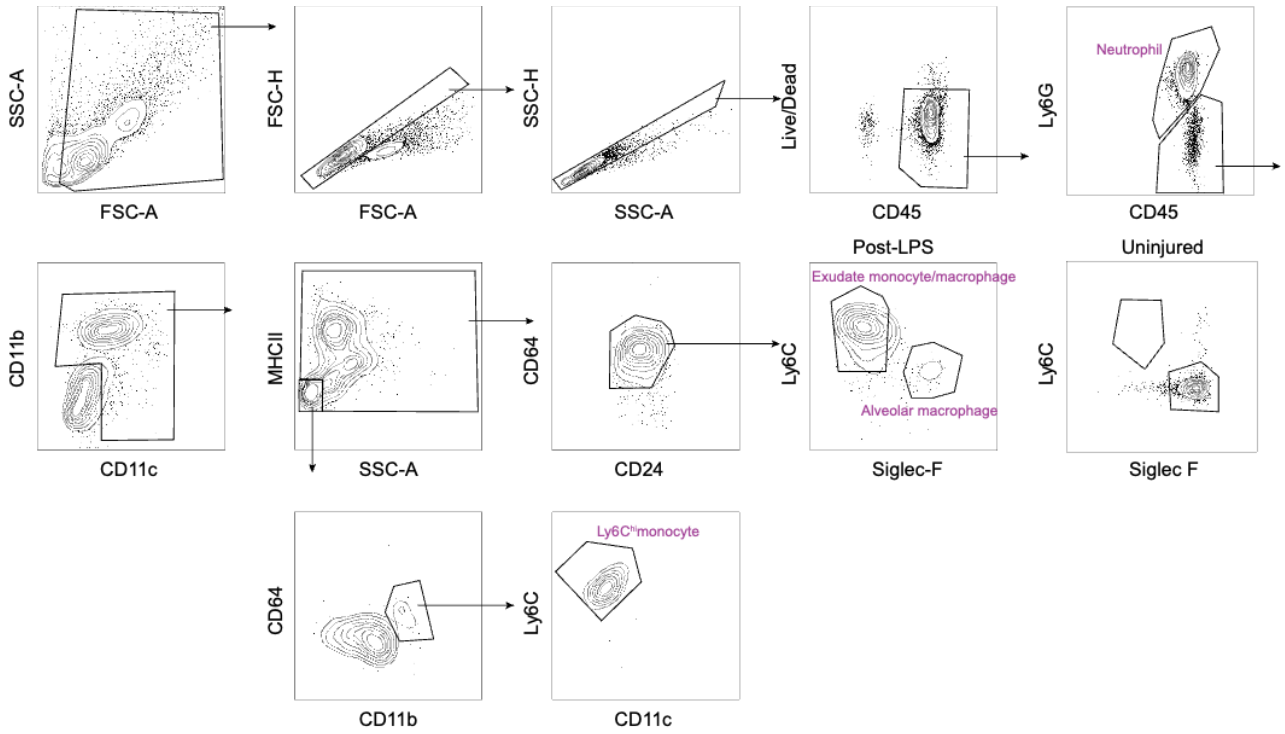


Figure S2. Exudate monocyte and macrophage flow cytometry panel performed on BAL. Exudate monocyte/macrophages in the BAL were assessed as previously described (15). Exudate monocyte/macrophage were identified within the myeloid (CD11b+ or CD11c+) population as MHCII^{+}/SSC^{hi}/CD64^{+}/Ly6C^{+}/Siglec-F^{-} events, and Ly6C^{hi} monocytes were identified within the myeloid population (CD11b^{+} or CD11c^{+}) as MHCII^{-}/SSC^{lo}/CD64/Ly6C^{hi} events. All populations gated using FMO controls. As shown, exudate monocyte/macrophage are not present in the BAL in uninjured lung but are present post-LPS (72 hours) indicating recruitment to the airspace under LPS administration.

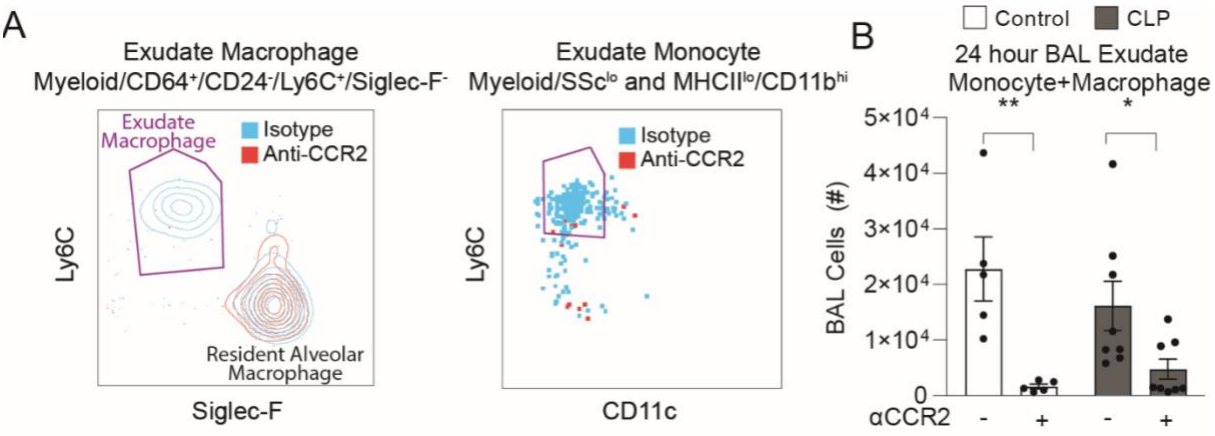


Figure S3. Anti-CCR2 treatment effectively depletes exudate Ly6C^{hi} monocytes and macrophages. Exudate monocyte/macrophages were assessed 24 hours after LPS administration following monocyte depletion in BAL fluid (A). Exudate monocyte/macrophage were identified (Figure S1), proportions shown for exudate monocyte/macrophage combined before and after depletion. 1 cohort shown, n = 5-8 per group. Mean ± SEM, post-hoc sidak t-test shown. * $p < 0.05$, ** $p < 0.01$. CLP, Cecal Ligation and Puncture. LPS, Lipopolysaccharide. BAL, bronchoalveolar lavage.

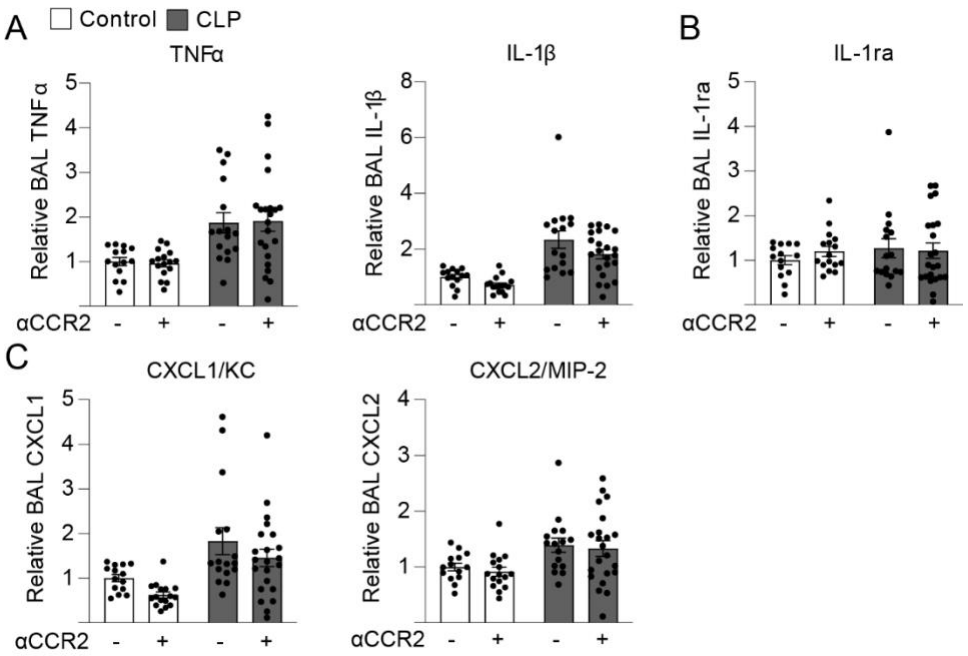


Figure S4. BAL inflammation following monocyte depletion. Lung inflammatory proteins were assessed in BAL 72 hours after LPS administration. Inflammatory proteins (A), anti-inflammatory proteins (B), and neutrophil chemokines shown (C). n = 4-8 per group, 3 cohorts. Relative BAL protein levels expressed relative to isotype treated control mice. Mean ± SEM shown. BAL, bronchoalveolar lavage. CLP, cecal ligation and puncture.

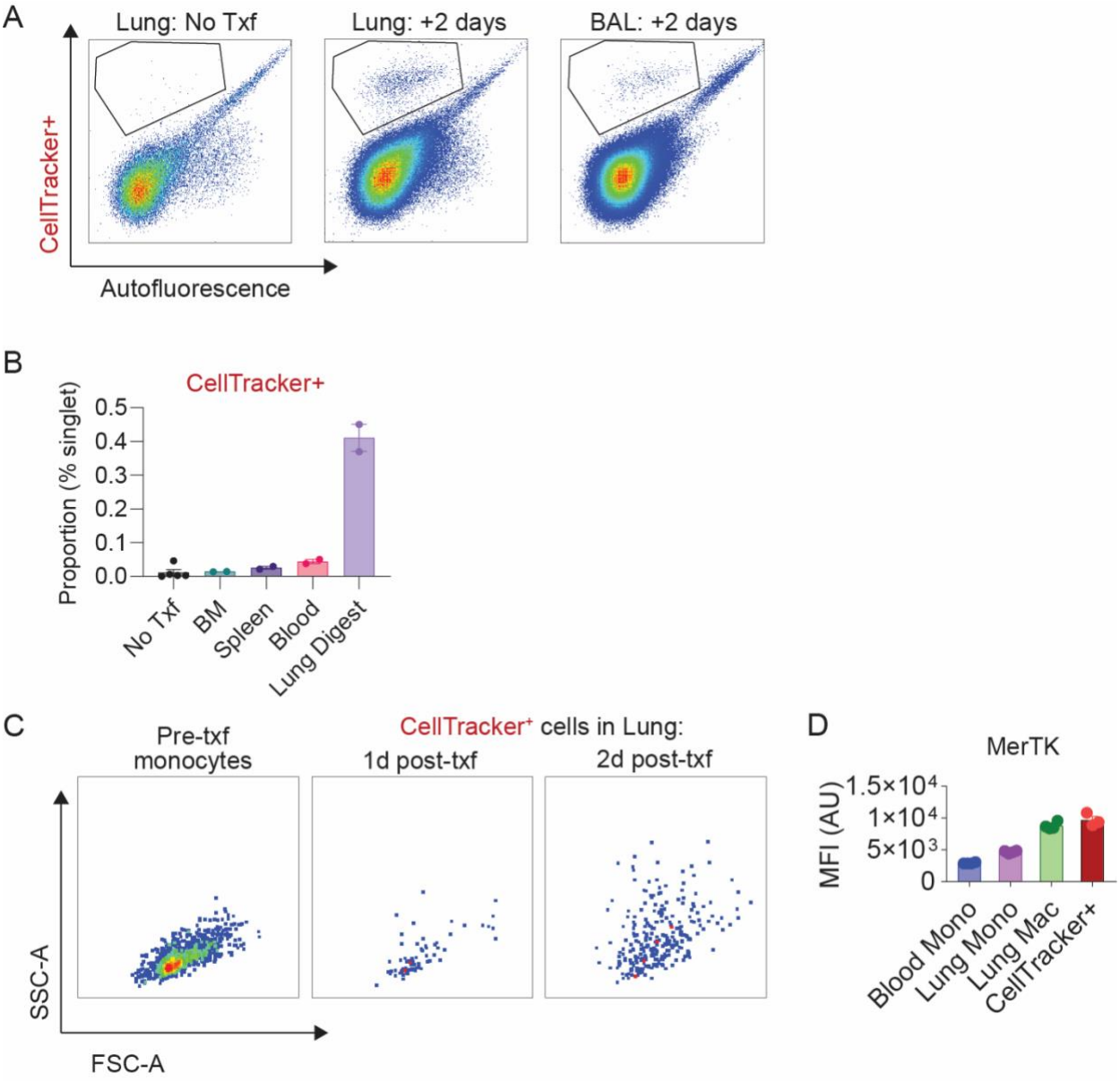


Figure S5. Verification of transferred monocyte migration to the lung and differentiation into lung macrophages. BM monocytes were isolated from *Ccr2*^{wt} mice, labeled with CellTracker dye, and transferred i.v. to *Ccr2*^{ko} mice at the time of i.n. LPS administration. Lung and BAL flow cytometry 2 days after transfer (A). CellTracker+ cell proportions across tissues 2 days after transfer (B). Scatter profiles (C) and MerTK staining (D) of transferred cells 2 days after transfer indicating macrophage differentiation in lung digest. Txf, transfer. MFI, median fluorescence intensity.

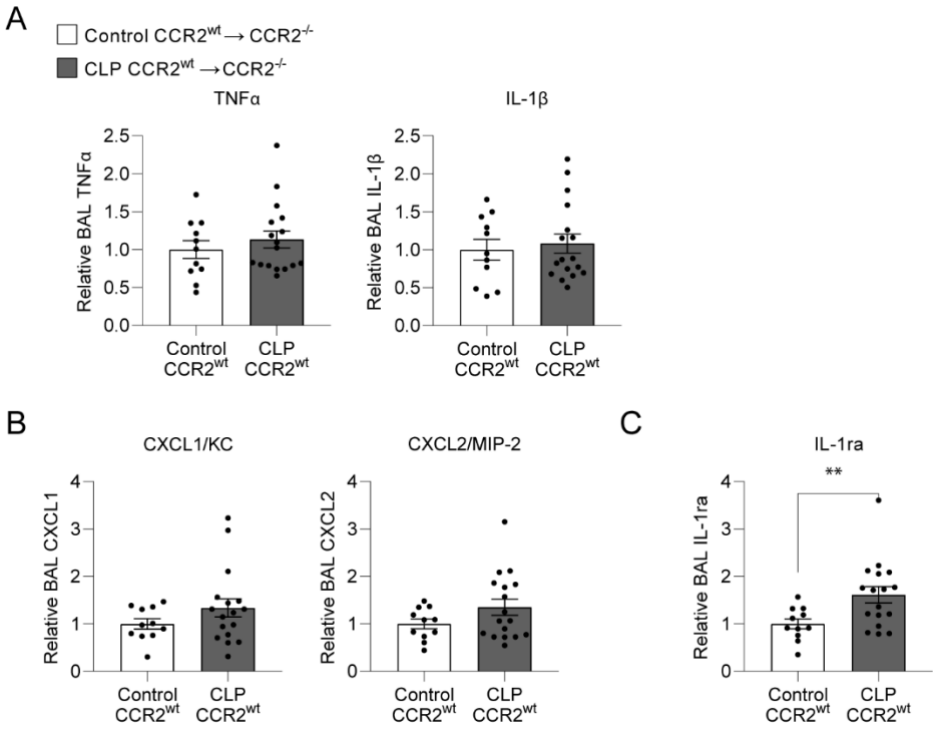


Figure S6. BAL inflammation following monocyte adoptive transfer. Lung inflammatory proteins were assessed 72 hours after adoptive transfer of monocytes. Inflammatory proteins (A), neutrophil chemokines (B), and anti-inflammatory proteins shown (C). Protein measurements expressed relative to the $CCR2^{wt}$ unoperated control transfer within each cohort. 3 cohorts shown, n = 3-6 per group. Mean ± SEM, Welch's t-test p-value shown. ** $p < 0.01$. CLP, Cecal Ligation and Puncture. BAL, bronchoalveolar lavage.

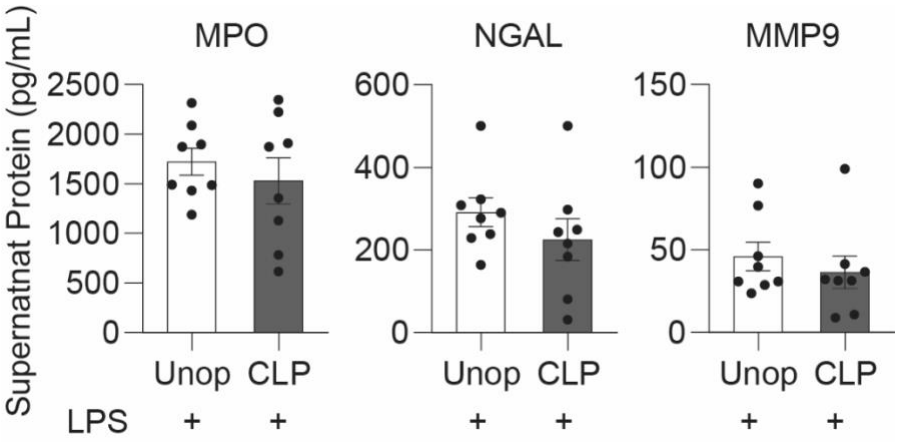


Figure S7. Monocyte supernatant degranulation markers. Monocytes from 3-wk post-CLP and control mice were stimulated with LPS ex vivo and supernatants collected.

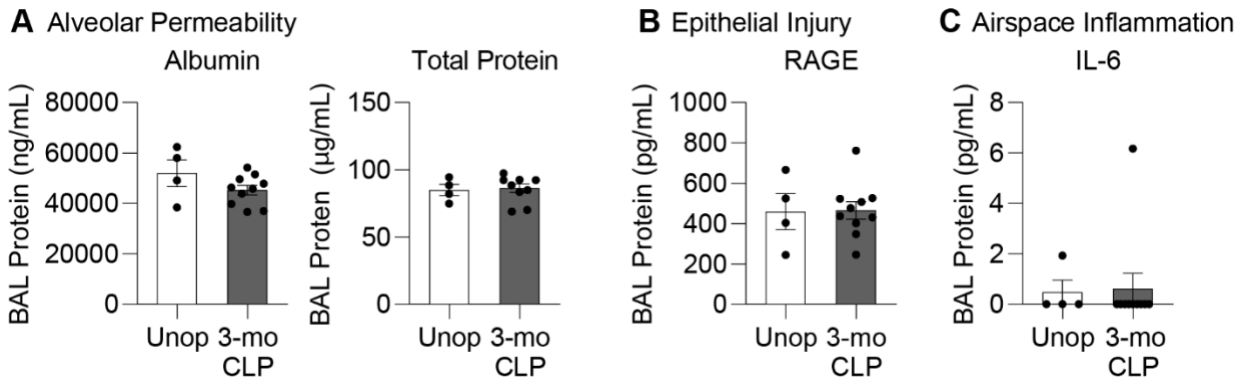


Figure S8. Baseline lung injury and inflammation 3 months post-CLP. BAL alveolar permeability (A), epithelial injury (B), and airspace inflammation (C).

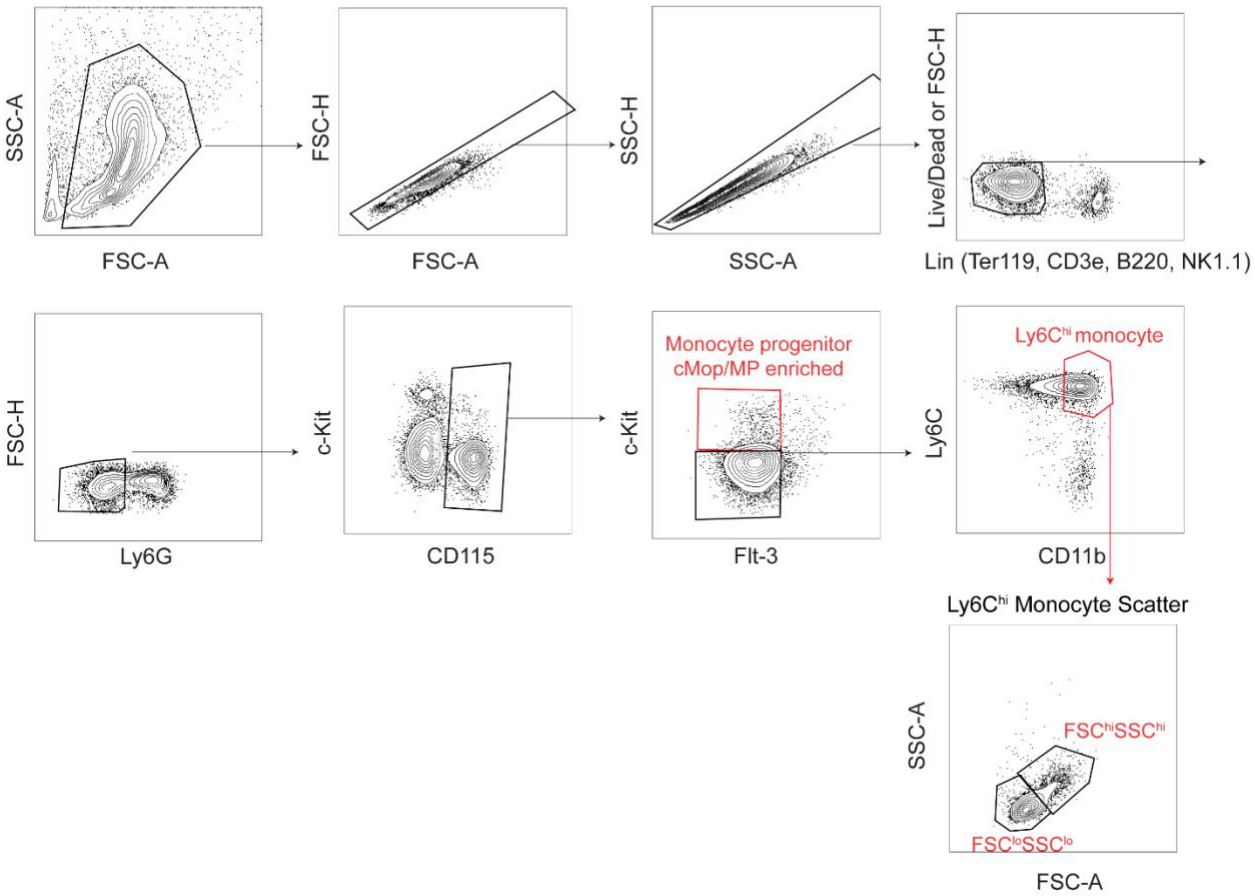


Figure S9. Bone marrow monocyte and progenitor flow gating strategy for flow sorting. Ly6C^{hi} monocytes and cMoP/MP populations (red boxes) were identified and sorted as previously described (16). All populations gated using FMO controls.

A

KEGG Term	Up Regulated in CLP	Down Regulated in CLP
HIF-1 signaling pathway	*Tlr4, Hif1a, Camk2d, Eno1, Pgk1, Ldha*	*Igf1, Flt1*
Oocyte meiosis	*Aurka, Mapk13, Plk1, Cdc25c, Ccnb2, Cdc20, Ccnb1, Camk2d*	*Igf1*
Glycerolipid metabolism	*Mboat1, Dgat2*	*Lpin1, Lpl*
Th17 cell differentiation	*Mapk13, Il21r, Jak3, Hif1a*	*Nfkbia, Nfkbie, Ebi3, Stat1*
PPAR signaling pathway	*Acsl3*	*Cd36, Cyp27a1, Lpl*
Toll-like receptor signaling pathway	*Lbp, Tlr4, Myd88, Mapk13*	*Nfkbia, Stat1, Cxcl10*
Focal adhesion		*Thbs1, Itga8, Itgb3, Pdgfb, Igf1, Flt1, Vav2*
Influenza A	*Tlr4, Myd88, Socs3*	*Nfkbia, Cxcl10, Stat1, Rsad2*

B

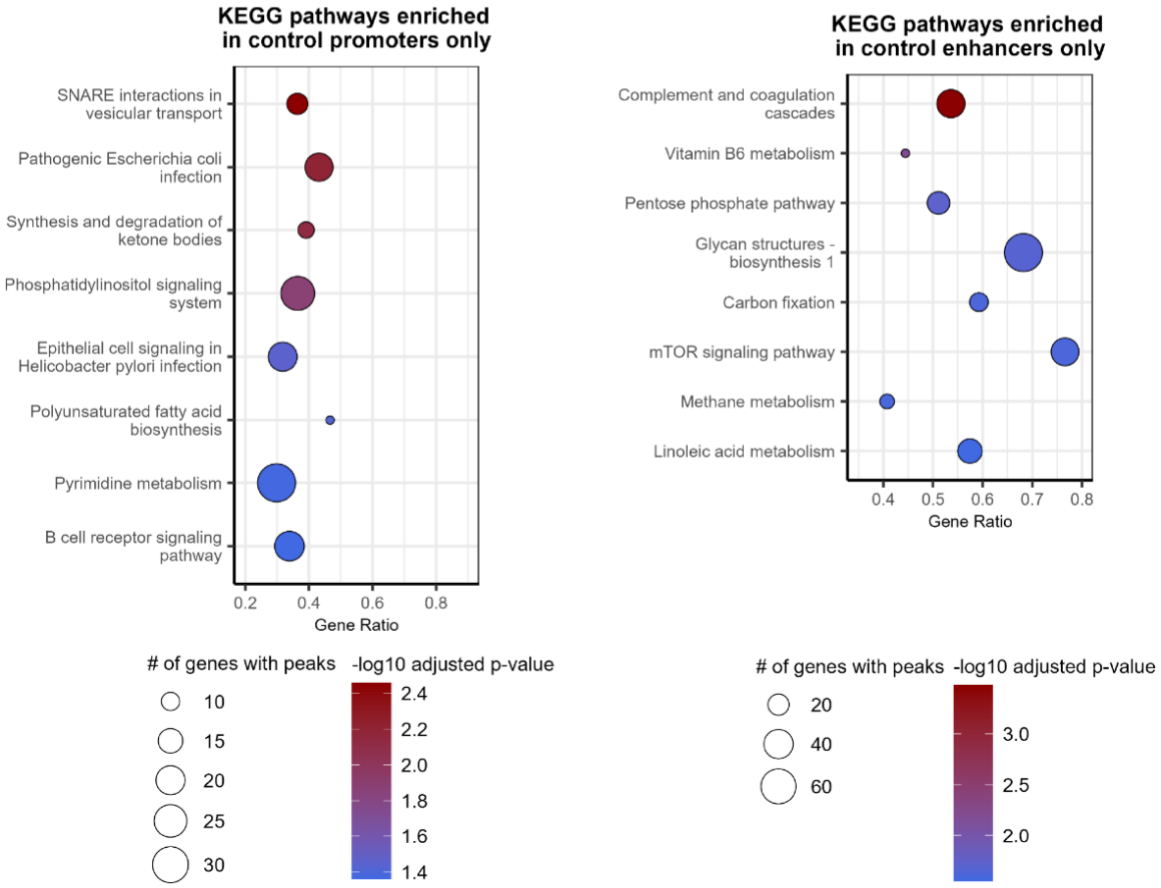


Figure S10. Differential pathway analysis and chromatin accessibility pathway enrichment in Ly6C^{hi} monocytes. RNA-seq pathway enrichment showing select enriched KEGG terms and associated genes (A). ATAC-seq pathway enrichment showing chromatin accessibility patterns in control mice (B). Promoters were defined as genomic regions < 1 kb from a transcription start site (TSS). Enhancers were defined as genomic regions > 1 kb from a TSS.

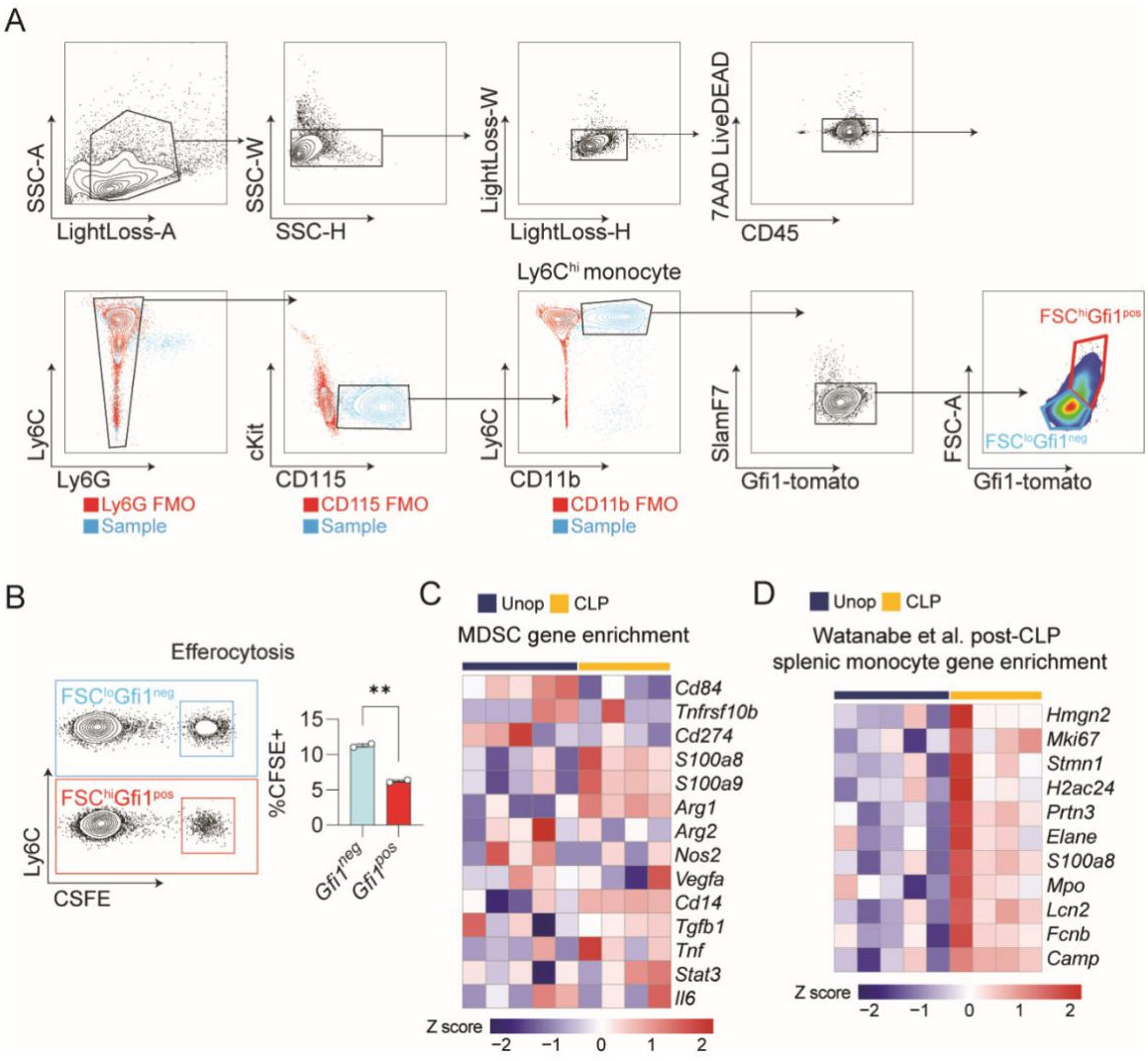
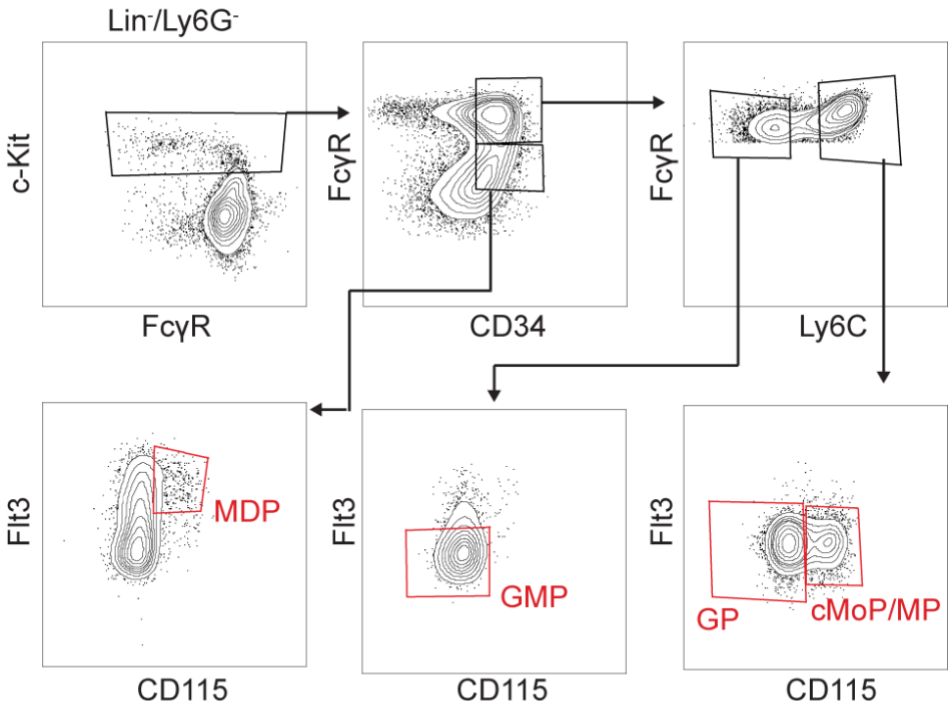


Figure S11. **Post-CLP bone marrow monocyte characterization.** Monocyte subset sorting panel to isolate GMP-derived Gfi1^{pos} and Gfi1^{neg} monocytes from the MDP-derived SlamF7 expressing population (A). Monocyte subset efferocytosis (B). MDSC gene enrichment (C), Watanabe et. al splenic monocyte cluster defining gene enrichment (D). MDSC, myeloid-derived suppressor cell.



	c-Kit	CD34	FcγR	Flt3	CD115	Ly6C
MDP	+	+	lo	+	+	-
GMP	+	+	hi	-	-	-
GP	+	+	hi	-	-	+
cMoP/MP	+	+	hi	-	+	+

Figure S12 Monocyte/myeloid progenitor flow panel(17)**.** MDP, monocyte-dendritic cell progenitor. GMP, granulocyte-monocyte progenitor. cMoP, MP, committed monocyte progenitors. GP, granulocyte progenitor.

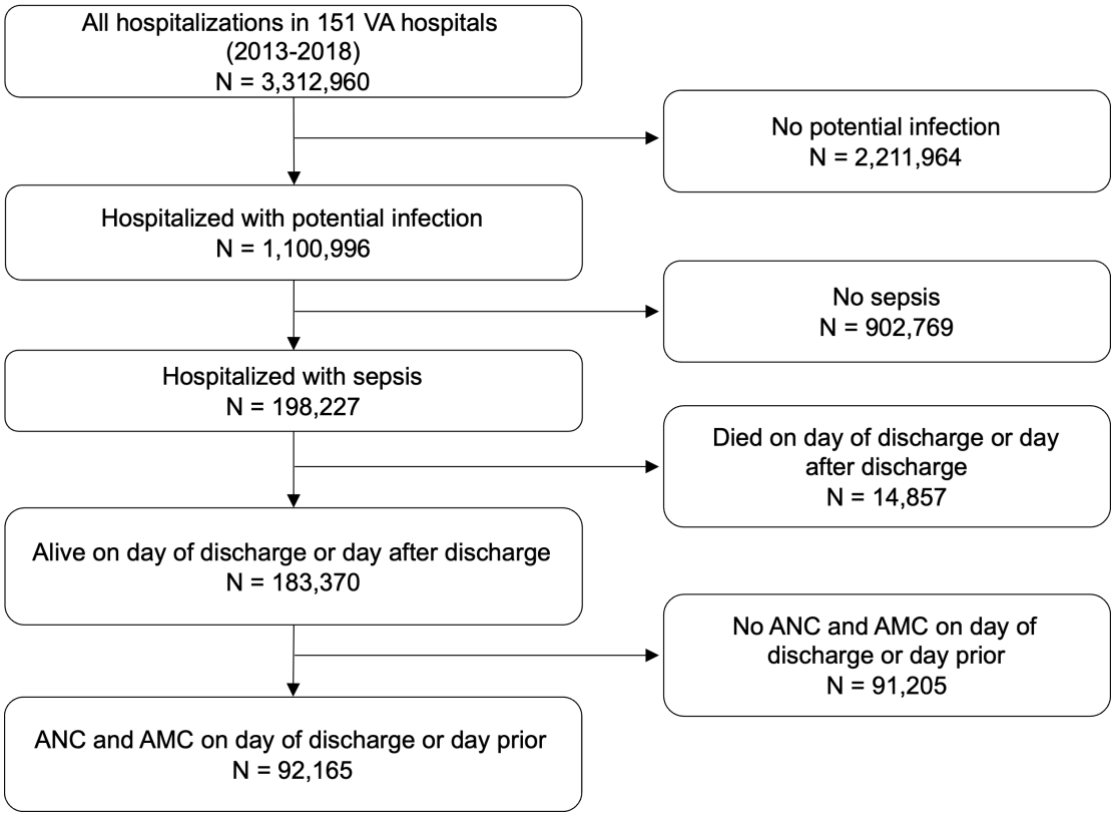


Figure S13. Consort Diagram of VA Hospitalizations. Hospitalizations with potential infection were defined as ≥2 SIRS criteria and treatment with antimicrobials within 48 hours of arrival. Hospitalizations for sepsis were defined, as in supplemental Table 1, as potential infection with continuation of antimicrobials for at least 4 days and ≥ 1 acute organ dysfunctions within 48 hours of arrival through the emergency department. ANC, absolute neutrophil count. AMC, absolute monocyte count.

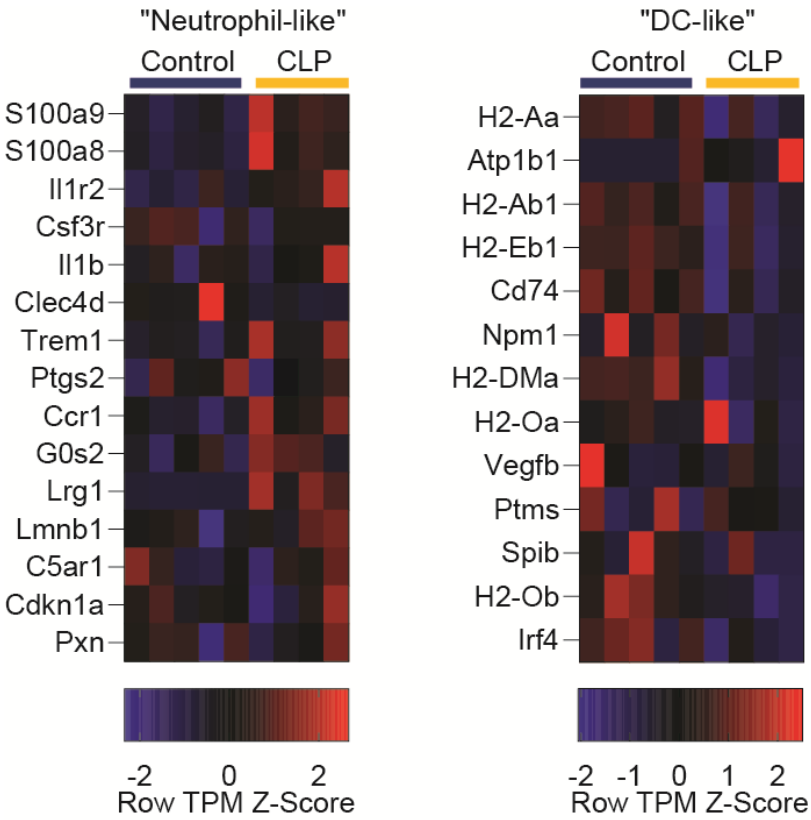


Figure S14. Conserved human-mouse signature(18) **in mouse Ly6C^{hi} monocytes.** Row TPM Z-score shown.

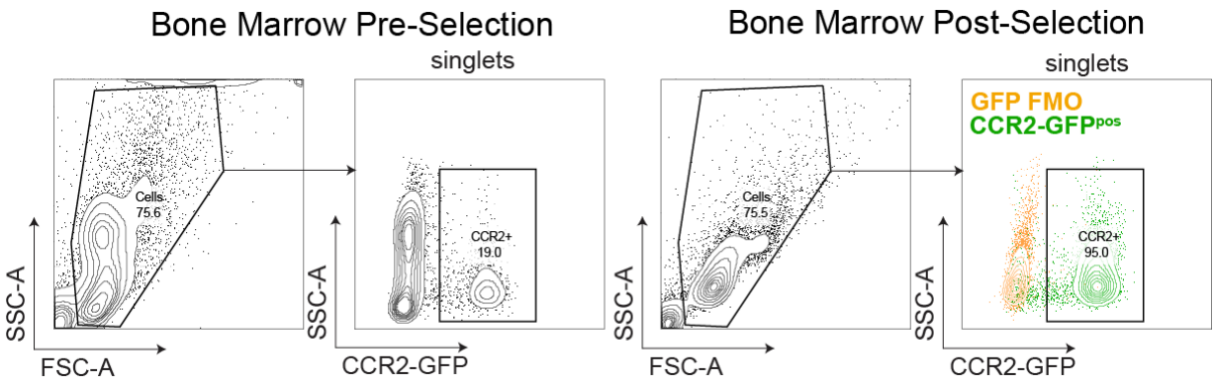


Figure S15. Monocyte purity of adoptively transferred monocytes following immunomagnetic selection.

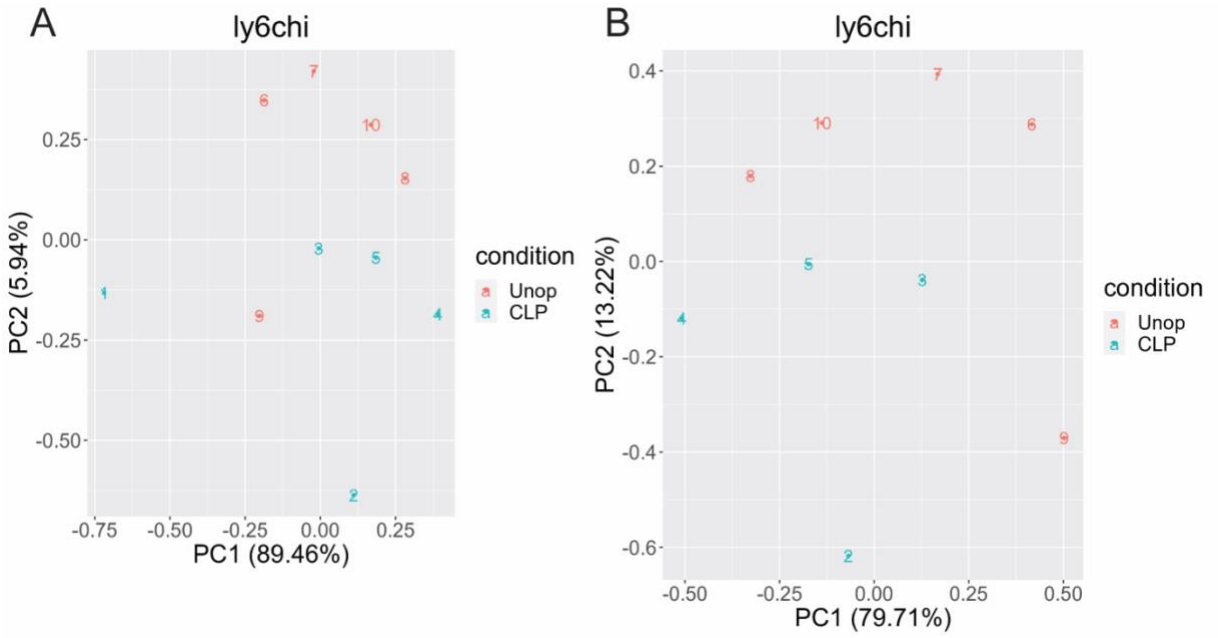


Figure S16. PCA plot of RNA-seq analysis performed on flow sorted Ly6C^{hi} monocytes. PCA plot shown before (A) and after (B) exclusion of a single outlier sample in the CLP group (sample #1).

Supplemental Table 1. Characteristics of Sepsis Cohort			
	Total Cohort n = 92165 (100.0)	**No mortality** n = 79600 (86.4)	**90-day all-cause mortality** n = 12565 (13.6)
Age, median (IQR)	68 (62, 76)	68 (61, 75)	72 (66, 83)
Sex, M, %	88811 (96.4)	76533 (96.1)	12278 (97.7)
Race, %			
Black	18622 (20.2)	16221 (20.4)	2401 (19.1)
White	65932 (71.5)	56887 (71.5)	9045 (72.0)
Other	2003 (2.2)	1782 (2.2)	221 (1.8)
Unknown	5463 (5.9)	4605 (5.8)	858 (6.8)
Comorbidity count, median (IQR)	7 (4, 9)	6 (4, 9)	8 (6, 10)
Select comorbid conditions, n (%)			
Any Diabetes	47522 (51.6)	41336 (51.9)	6186 (49.2)
Chronic pulmonary disease	43377 (47.1)	36790 (46.2)	6587 (52.4)
CKD	33130 (35.9)	27592 (34.7)	5538 (44.1)
Diabetes with complication	31843 (34.5)	27683 (34.8)	4160 (33.1)
Congestive heart failure	29992 (32.5)	24636 (30.9)	5356 (42.6)
Any Cancer	23721 (25.7)	18338 (23)	5383 (42.8)
Liver disease	17237 (18.7)	14315 (18)	2922 (23.3)
Neurologic disease	16561 (18.0)	13463 (16.9)	3098 (24.7)
Metastatic cancer	6646 (7.2)	4202 (5.3)	2444 (19.5)
Rheumatoid Arthritis/Collagen Vascular Diseases	4022 (4.4)	3473 (4.4)	549 (4.4)
Acute organ dysfunction count, median (IQR)	1 (1, 2)	1 (1, 2)	1 (1, 2)
Acute organ dysfunctions, n (%)			
Renal	57142 (62.0)	48894 (61.4)	8248 (65.6)
Elevated lactate	39523 (42.9)	33993 (42.7)	5530 (44.0)
Hematologic	10646 (11.6)	8544 (10.7)	2102 (16.7)
Hepatic	11878 (12.9)	9976 (12.5)	1902 (15.1)
Circulatory (vasopressor use)	6625 (7.2)	5377 (6.8)	1248 (9.9)
Respiratory (mechanical ventilation)	4093 (4.4)	3326 (4.2)	767 (6.1)
ICU admission, n (%)	26513 (28.8)	21745 (27.3)	4768 (37.9)
Hospital LOS, median (IQR, days)	6 (4, 10)	6 (4, 9)	8 (5, 12)
Discharge blood parameter, median (IQR)			
ANC (10^3/μL)	5.64 (3.83, 7.88)	5.55 (3.80, 7.70)	6.38 (4.20, 9.04)
AMC (10^3/μL)	0.70 (0.50, 0.93)	0.70 (0.50, 0.93)	0.70 (0.47, 0.97)

Comorbidity count determined using 30 Elixhauser comorbidities (19).

ANC, absolute neutrophil count. AMC, absolute monocyte count.

Supplemental Table 2. Sepsis Hospitalization Criteria – Veterans Affairs Hospital Data		
Broad Criteria‡	**Specific Criteria**	**References**
Admission through the emergency department	N/A	
Suspected infection	2+ systemic inflammatory response criteria (SIRS),	(20,21)
	Initiation of systemic antimicrobials (oral or intravenous) within 48 hours of ED arrival,	
	AND Continuation of antimicrobials for at least 4 days, inclusive of antibiotics prescribed at discharge to be completed at home	
≥ 1 acute organ dysfunction within 48 hours of emergency department arrival	acute renal dysfunction†	(20)
	acute liver dysfunction†	
	acute hematologic dysfunction†	
	lactate > 2.0 mmol/L	
	receipt of invasive mechanical ventilation	
	receipt of systemic vasopressors	
†Acute renal, liver, and hematologic dysfunction were defined as worsening of creatinine, total bilirubin, or platelet count respectively from baseline. Baseline was defined as the best laboratory value during hospitalization or the preceding 6 months (20). ‡Broad criteria for sepsis hospitalization are adapted from the CDC definition for an adult sepsis event (ASE)		

Supplemental Table 3: Lab Data Check Table (Pre-Trim):
Use the last CBC parameters of hospitalization that occur on day of discharge or day prior,
AFTER excluding non-physiologic labs (values ≤ 0 or ≥ 300 x 10^3 cells/µl)
BEFORE excluding top/bottom percentile

CBC Parameter	Total measurements	% of hospitalizations	Mean	Min	1st%ile	25%ile	Median	75%ile	99th%ile	Max
ANC	103171	56.3	6.27	0.00	0.10	3.80	5.65	7.96	18.50	195.10
AMC	104020	56.7	0.76	0.01	0.08	0.50	0.70	0.95	2.10	135.50

Supplemental Table 4: Lab Data Check Table (POST-Trim):
Use the last CBC parameters of hospitalization that occur on day of discharge or day prior,
AFTER excluding non-physiologic labs
AFTER excluding top/bottom percentile

CBC Parameter	Total measurements	% of hospitalizations	Mean	Min	1st%ile	25%ile	Median	75%ile	99th%ile	Max
ANC	101324	55.3	6.12	0.10	0.50	3.80	5.63	7.90	15.91	18.50
AMC	102130	55.7	0.74	0.08	0.10	0.50	0.70	0.93	1.80	2.10

References

1. Martin M. Cutadapt removes adapter sequences from high-throughput sequencing reads. *EMBnet.journal*. 2011;17(1):10.
2. Dobin A, et al. STAR: Ultrafast universal RNA-seq aligner. *Bioinformatics*. 2013;29(1):15-21.
3. Kim D, et al. Graph-based genome alignment and genotyping with HISAT2 and HISAT-genotype. *Nat Biotechnol*. 2019;37(8):907-915.
4. Li B, Dewey CN. RSEM: accurate transcript quantification from RNA-Seq data with or without a reference genome. *BMC Bioinformatics*. 2011;12(1):323.
5. Anders S, et al. HTSeq-A Python framework to work with high-throughput sequencing data. *Bioinformatics*. 2015;31(2):166-169.
6. Love MI, et al. Moderated estimation of fold change and dispersion for RNA-seq data with DESeq2. *Genome Biol*. 2014;15(12):550.
7. Ulgen E, et al. PathfindR: An R package for comprehensive identification of enriched pathways in omics data through active subnetworks. *Front Genet*. 2019;10(SEP):425394.
8. Corces MR, et al. An improved ATAC-seq protocol reduces background and enables interrogation of frozen tissues. *Nat Methods*. 2017;14(10):959-962.
9. Li H, et al. The Sequence Alignment/Map format and SAMtools. *Bioinformatics*. 2009;25(16):2078-2079.
10. Quinlan AR, Hall IM. BEDTools: A flexible suite of utilities for comparing genomic features. *Bioinformatics*. 2010;26(6):841-842.
11. Zhao N, Boyle AP. F-Seq2: Improving the feature density based peak caller with dynamic statistics. *NAR Genomics Bioinforma*. 2021;3(1):1-8.
12. Lee CT, et al. Poly-Enrich: count-based methods for gene set enrichment testing with genomic regions. *NAR Genomics Bioinforma*. 2020;2(1):1-13.
13. Bailey TL, Grant CE. SEA: Simple Enrichment Analysis of motifs. *bioRxiv*. Published online August 24, 2021:2021.08.23.457422.
14. Grant CE, et al. FIMO: Scanning for occurrences of a given motif. *Bioinformatics*. 2011;27(7):1017-1018.
15. Yu YRA, et al. A Protocol for the Comprehensive Flow Cytometric Analysis of Immune Cells in Normal and Inflamed Murine Non-Lymphoid Tissues. Mueller SN, ed. *PLoS One*. 2016;11(3):e0150606.
16. Hettinger J, et al. Origin of monocytes and macrophages in a committed progenitor. *Nat Immunol 2013 148*. 2013;14(8):821-830.
17. Yáñez A, et al. Granulocyte-Monocyte Progenitors and Monocyte-Dendritic Cell Progenitors Independently Produce Functionally Distinct Monocytes. *Immunity*. 2017;47(5):890-902.e4.

18. Zilionis R, et al. Single-Cell Transcriptomics of Human and Mouse Lung Cancers Reveals Conserved Myeloid Populations across Individuals and Species. *Immunity*. 2019;50(5):1317-1334.e10.

19. Denstaedt SJ, et al. Blood count derangements after sepsis and association with post-hospital outcomes. *Front Immunol*. 2023;14(February):1-11.

20. Wayne MT, et al. Measurement of Sepsis in a National Cohort Using Three Different Methods to Define Baseline Organ Function. *Ann Am Thorac Soc*. 2021;18(4):648-655.

21. Bone RC, et al. Definitions for sepsis and organ failure and guidelines for the use of innovative therapies in sepsis. The ACCP/SCCM Consensus Conference Committee. American College of Chest Physicians/Society of Critical Care Medicine. *Chest*. 1992;101(6):1644-1655.